06

Nanocomposite tensoresistive elements based on carbon nanomaterials for wearable electronics

© K.D. Popovich,[1,2] V.V. Suchkova,[1,2] D.I. Ryabkin,[1,2] A.A. Pugovkin,[1,2] E.A. Gerasimenko,[3] D.V. Telyshev,[1,2] S.V. Selishchev,[1] A.Yu. Gerasimenko[1,2]

[1]Institute of Biomedical Systems, National Research University „Moscow Institute of Electronic Technology“, 124498 Moscow, Zelenograd, Russia
[2]Institute of Bionic Technologies and Engineering, I.M. Sechenov First Moscow State Medical University, 119991 Moscow, Russia
[3]Orthopedic Department, State Autonomous Health Care Institution of Moscow „Dental Clinic No. 35“, 124365 Moscow, Zelenograd, Russia
e-mail: kristal_p@mail.ru

Received December 13, 2024
Revised December 13, 2024
Accepted December 13, 2024

The investigation focused on the potential application of flexible electrically conductive elements in the domain of wearable electronics and motor activity monitoring, encompassing the use in limbs, gesture recognition, and diagnostics of temporomandibular joint movements. Multi-walled carbon nanotubes, when incorporated into a biopolymer matrix, were utilized as an active electrically conductive layer. To create nanocomposite tensoresistive elements, the active layer was formed between flexible soft silicone substrates. The structural characteristics of the developed elements were investigated, electrical conductivity and mechanical properties were evaluated, and their performance for various biomedical applications was verified.

Keywords: strain sensitivity, multi-walled carbon nanotubes, silicone, gesture recognition, temporomandibular joint.

DOI: 10.61011/TP.2025.05.61121.451-24

Introduction

Flexible strain sensors represent their own important class of sensor devices that have found wide application in various fields, in particular, in biomedicine [1,2], robotics [3,4], automotive industry [5] and virtual reality for tracking user motion [6]. They are capable of detecting both small and large deformations due to their high flexibility and softness. Frequency, resistive, and capacitive strain and pressure sensors are widely used in the field of wearable electronics [7,8]. Resistive sensors are more sensitive and less susceptible to interference than capacitive sensors fabricated using the same technology [9].

Strain gauges are typically made of functional materials integrated into flexible substrates. For resistive sensors, such materials are carbon (carbon nanotubes (CNTs) [10], graphene [11]), metals [12] (metal particles, nanowires, etc.), various electrically conductive polymers [13] (polypyrrole, polyaniline, polystyrene sulfate). For flexible carrier materials/substrates (flexible matrices) the elastomers were used most often: rubber [14], polydimethylsiloxane (PDMS) [15], silicone Ecoflex [10], polyethylene terephthalate (PETP) [16], as well as other synthetic and other natural polymers.

Among all varieties of electrically conductive functional materials, CNTs attract much attention. These nanomaterials, used in combination with polymer matrices, have unique mechanical and electrical properties, making them an ideal choice for creating sensitive and durable sensors [17]. Polymers, in turn, are distinguished by easy manufacturing process, cost-effectiveness and flexibility. In addition, the physical properties of polymers, such as hardness and elasticity, can be easily adjusted over a wide range, allowing to design the materials with the best properties for specific applications. All this makes the combination of CNTs with polymers very promising for the development of the high-end materials and technologies used in sensors and electronics.

CNTs have a unique ability to interact with various biomolecules due to which their biocompatibility rises significantly. Recent studies confirm the practical absence of cytotoxicity of CNTs when used in low concentrations [18,19]. The integration of CNTs into polymer matrices makes it possible to create nanocomposites with high electrical conductivity at very low concentrations of CNTs, which makes their use cost-effective and reasonable [20]. The resulting nanocomposites have the ability to form percolation networks that can self-repair after deformation, making CNTs an ideal material for the development of highly efficient flexible strain sensors capable of withstanding stretching and bending.

In this work, the tensoresistive characteristics of nanocomposite elements based on structured CNT networks in a silicone matrix were investigated. The variations in electrical resistance depending on bending and stretching strain were observed in the studied samples. The results

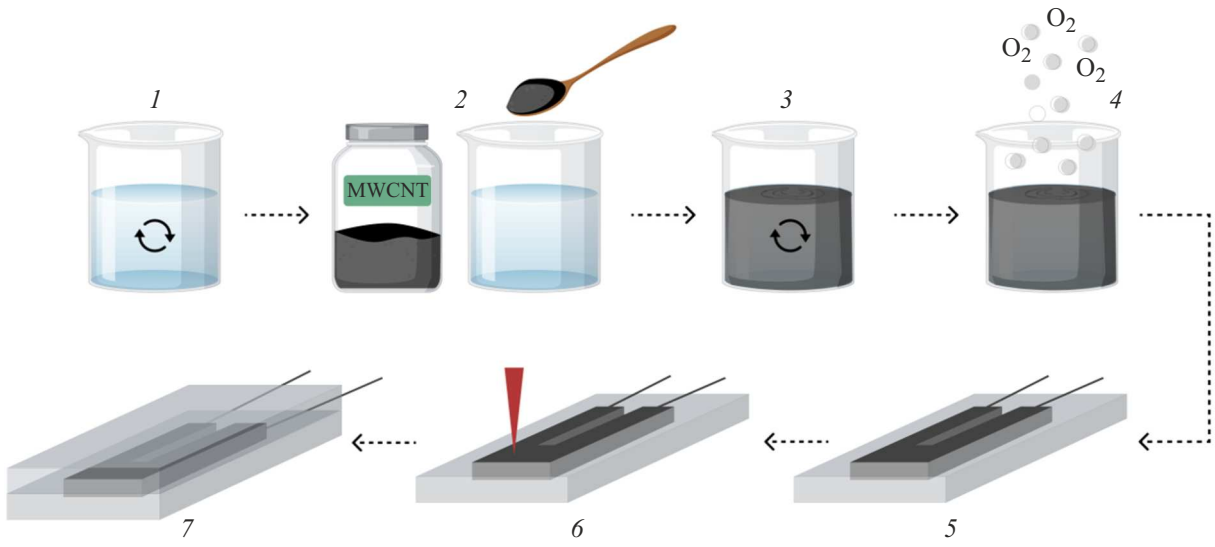

Figure 1. Fabrication of composite tensoresistive elements based on MWCNT and silicone: *1* — mixing of the two-component silicone Ecoflex; *2* — addition of MWCNT into polymer solution; *3* — mixing of the obtained dispersion media; *4* — degassing until full removal of air bubbles; *5* — integration of copper wires into active layer; *6* — polymerization of active layer and further laser structuring of the conducting nets; *7* — isolation of active layer by formation of additional silicone substrate.

obtained indicate the potential application of the designed nanocomposite tensoresistive elements in flexible sensors for measuring various types of mechanical deformations in wearable electronics.

1. Materials and research methods

Section 1 outlines the materials used, technical characteristics and method of manufacturing the tensoresistive elements. The morphology of the grown structures was studied by scanning electron microscopy (SEM). A method for studying strain resistance and operability is described.

1.1. Materials used

Multi-walled carbon nanotubes (MWCNT) embedded in a silicone matrix were used as the active layer of the tensoresistive elements. MWCNT (OOO „NanoTechCenter“, Tambov, Russia) powder was synthesized by CVD method and characterized by the following parameters: outer diameter — 30–80 nm, inner diameter — 10–20 nm, length of $\geq 20\,\mu$m, specific surface — $\geq 200\,m^2/g$, volumetric density 0.025–0.06 g/cm^3, thermal stability of up to 600 °C.

The two-component elastomer Ecoflex 00-10 (Smooth-On Inc., Macungie, Pennsylvania, USA) had dynamic viscosity in mixed state of 14 Pa, Young's modulus at 100 % elongation of 0.06 MPa, density of 1.04 g/cm^3, operating temperature range of 19 °C up to 232 °C. At the first stage of polymerization, copper wires were included in the samples.

1.2. Fabrication of tensoresistive elements based on MWCNT and silicone

For the formation of the tensoresistive elements a photopolymer mold was printed on 3*D*-printer. In our case, the shape had the form of a rectangle, with dimensions $3.5 \times 1.5 \times 2$ mm, and had an inner U-shaped semi-axis with dimensions $3 \times 1.2 \times 1$ mm. The next step was to prepare an active layer consisting of a MWCNT and silicone (Fig. 1). At the first stage, MWCNT was added to silicone in the liquid phase at a concentration of 3 wt.%. The resulting mixture of components was thoroughly mixed with a magnetic stirrer for at least 5 min to evenly distribute the nanotubes in silicone. To remove the air microbubbles of formed as a result of mixing, the mixture was placed in XFL020 vacuum chamber (France Etuves) and the degassing process took place until the air bubbles were completely removed. Next, nanocomposite tensoresistive elements were fabricated. For this purpose the mixture of MWCNT and silicone was placed into a U-shaped hollow part of the mold. Copper wires were integrated in the active layer to connect to the electronic unit and check its operability. After full polymerization, the obtained samples were subjected to laser structuring and laser radiation treatment to reduce resistance values, form welded joints between nanotubes, and form a structured conductive network of MWCNTs. A pulsed fiber Yb-laser with a wavelength of 1064 nm was used, the radiation power was selected experimentally and was 12 W, the irradiation time was 2 min. The energy density was 0.5 J/cm^2 with a pulse duration of 100 ns, a pulse repetition rate of — 30 kHz and a processing speed of — 450 mm/s.

1.3. Studying the structure of active layer

The structure of the active layer based on MWCNT and silicone was studied using a scanning electron microscope FEI Helios NanoLab 650 (FEI Ltd) with the following parameters: accelerating voltage 5 kV, electron probe current 50 pA. Vacuum chamber pressure was $3.9 \cdot 10^4$ Pa.

1.4. Study of electrophysical properties of active layer

The effect of MWCNT concentration and laser structuring on electrical resistance of prepared tensoresistive elements as rectangular nanocomposites with dimensions $3.5 \times 1.5 \times 1$ cm and MWCNT concentration of 2, 3 and 4 wt.% was estimated. Electrical resistance values were measured using multimeter UT33A+ (UNI-T) before and after laser structuring for each concentration of MWCNT. A pulsed ytterbium optical fiber laser with a wavelength of 1064 nm and a power of 12 W was used, the laser exposure time was 2 min.

1.5. Investigation of strain sensitivity and mechanical characteristics of the active layer

Strain sensibility or strain gauge resistivity of the sensor — its response to the deformation that manifests itself in the variation of the active layer resistance. The faster and the more the resistance varies, the higher the strain sensibility is. The strain sensitivity of the active MWCNT-based layer in a silicone polymer matrix is determined with respect to stretching. The calculations were carried out using formula (1):

$$S_l = \frac{\Delta R_l \cdot l_0}{R_0 \cdot \Delta l}, \tag{1}$$

where ΔR — absolute change of resistance, R_0 — initial resistance of element, l_0 — initial length of element, Δl — absolute change of length. To determine the strain sensitivity of the active layer, the prepared tensoresistive element was fixed in a vise and stretched, its elongation (in 5 mm increments) and resistance were recorded. After that, the value of the sensitivity coefficient at maximum tension was calculated.

In order to predict how the active layer behaves under various loads and operating conditions, it is necessary to study its mechanical properties. These properties include ultimate strength and modulus of elasticity.

The ultimate strength was found from the formula (2):

$$\sigma = \frac{P_{\max}}{F_0}, \tag{2}$$

where $P_{\max}$ —maximum load applied to the sample, F_0 — initial cross-sectional area of the sample.

The modulus of elasticity was found from the formula (3):

$$E = \frac{F \cdot l}{S \cdot \Delta l}, \tag{3}$$

where ifx26xe — applied force, l — initial length of the sample, S — cross-sectional area of the sample, Δl — increment of the sample length.

2. Results and discussion

Section 2 gives an insight on the structure of the resulting active MWCNT-based layer. The section outlines the strain sensitivity, mechanical properties and various fields of application (monitoring of limb and jaw joint motor activity) that had been tested.

2.1. Internal structure of active layer

The MWCNT-based active layer was irradiated by laser pulses during formation of the assembly layer based on MWCNT and silicone. This led to a partial burnout of the silicone layer, which reduced the electrical resistance by changing the filler/matrix ratio. A CNT net was formed in the material. The differences in the net appearance are clearly seen before (Fig. 2, *a, b*) and after (Fig. 2, *c, d*) laser structuring.

Laser structuring helped to purify the surface of the nanotubes, making the network more homogeneous and sparse. This is an important factor, since sparse conductive nets provide a higher sensitivity to deformation. The nanotubes formed long couplings with a length of more than 100 nm over the entire volume of the material (Fig. 2, *d*), which ensured functional characteristics and efficient operation of the active layer due to their high electrical conductivity and tensoresistive properties.

Higher-magnification SEM images allowed to study the structure of the conductive net in details. The internal structure was studied for the active layer prepared without laser structuring (Fig. 3, *a*) and with laser structuring (Fig. 3, *b*). After laser structuring, the MWCNT nets structure changes. Large clusters are divided into smaller ones, which increase the number of clusters and decrease their average size. The conductive MWCNT net has become less complex after laser structuring, with a predominance of nanotube junction regions. For sensors, it is preferable to use a more sparse network, since it provides lower resistance hysteresis. This happens because a more sparse net is stretched more evenly and the restructuring of the conductive net becomes more stable due to the absence of large numbers of conductive paths. This means that there is less chance of an accidental contribution to the conductivity of untangled or randomly coupled nanotubes. Fig. 3, *c, d* shows the welding sites of nanotubes at higher magnification, the arrows show the points of contact between the MWCNTs.

2.2. Electrical and mechanical characteristics, strain sensitivity

The electrophysical properties of the prepared nanocomposite elements obtained with and without laser structuring

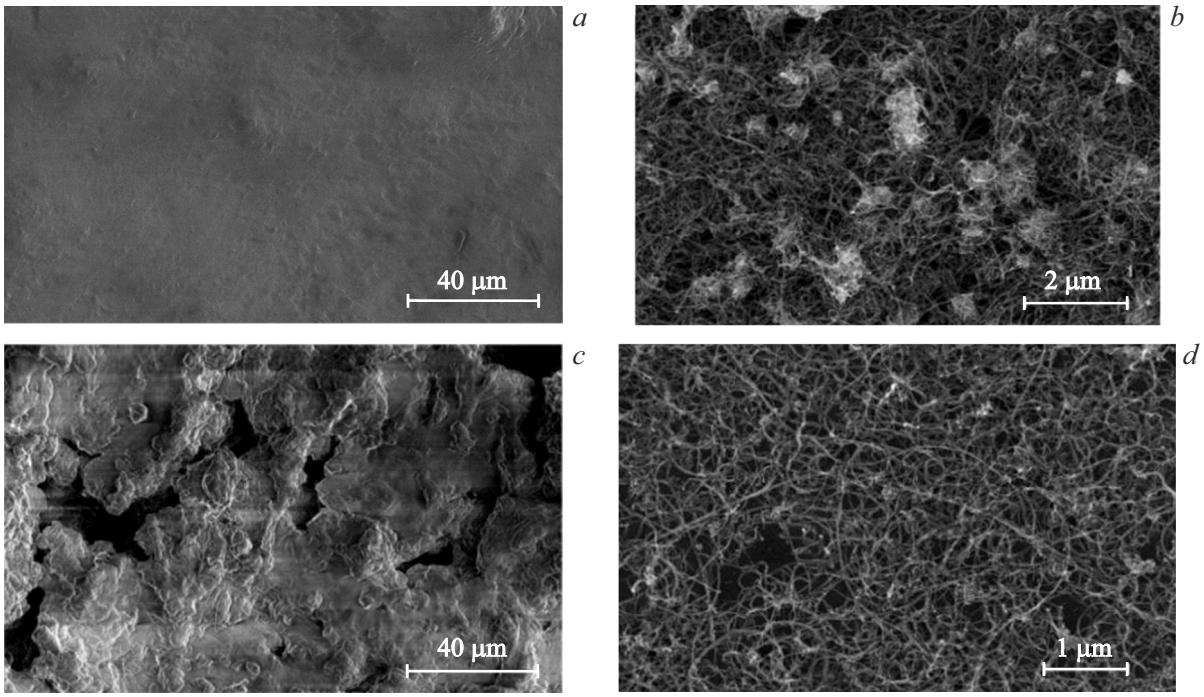

Figure 2. SEM images of the active layer of composite tensoresistive element based on MWCNT and silicone without laser structuring at various magnification (a, b) and with laser structuring (c, d).

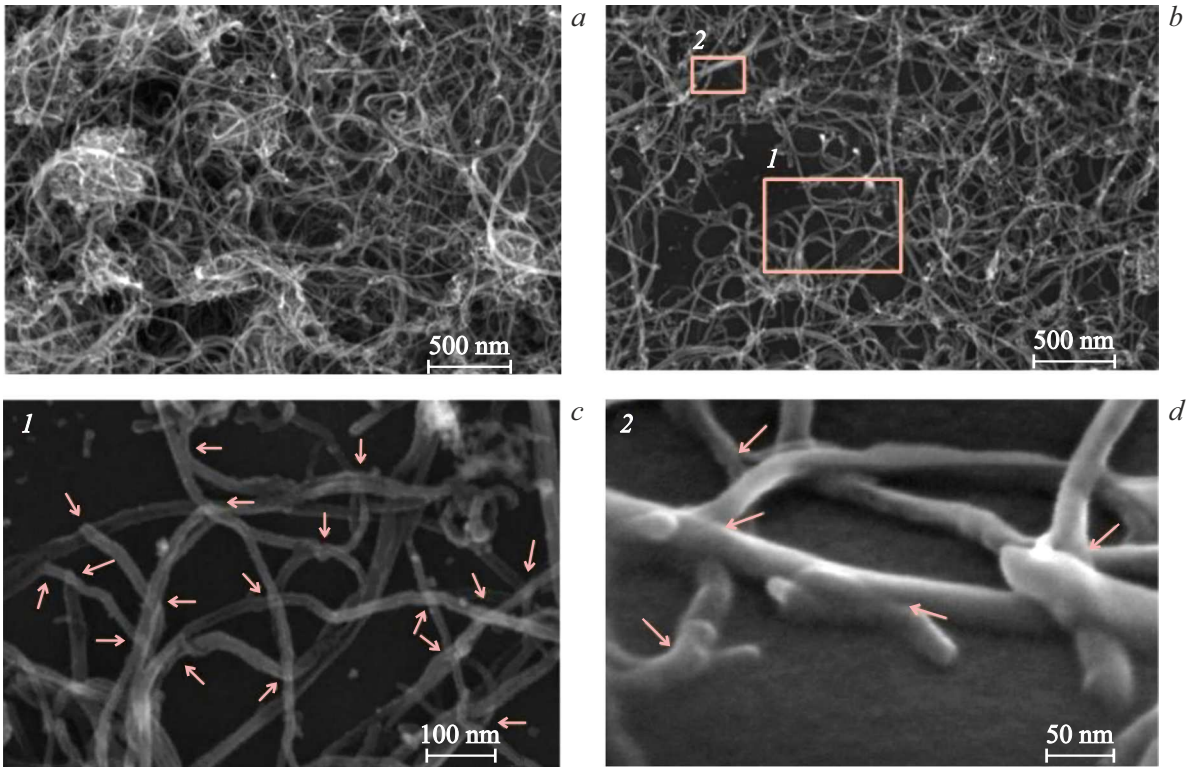

Figure 3. Internal structure of active layer of the composite tensoresistive composite element, fabricated without laser structuring (a) and with laser structuring (b–d). Image of area *2* was made at an angle 52°. The arrows indicate the welded sections of nanotubes formed as a result of laser structuring.

Comparison of the initial resistance of the active layer of prepared nanocomposite elements based on MWCNT and silicone

MWCNT concentration, wt.%	R_0 for laser structuring	R_0 after laser structuring
< 2	$> 1\,M\Omega$	
2	102 kΩ	65 kΩ
3	20 kΩ	3 kΩ
4	6 kΩ	0.5 kΩ
> 4	–	–

were compared using different concentrations of nanotubes 2, 3.4 wt.% (see table).

The rise of MWCNT concentration above 4 wt.% greatly increases the viscosity of the material consisting of MWCNT and silicone. This affects the homogenization of MWCNT in silicone during the preparation of the sensitive material of the active layer. If MWCNT concentration is below 2 wt.% it leads to higher resistance of the fabricated active layer above 1 MΩ. Such high values lead to difficulties in detection of resistance changes and are unacceptable for the design of biomedical applications for detecting the motor activity. If nanocomposites with a concentration of MWCNT of 2 wt.% are exposed to higher laser power, then silicone in the active sensing layer overheats and collapses, which reduces the performance of the tensoresistive element.

The initial electrical resistance of laser-prepared nanocomposite elements is ~ 3 kΩ (without deformation) at concentration of nanotubes 3 wt.%. For comparison, in a similar fabrication process without laser structuring, the active layer had significantly higher resistance values, in this case ifx36xe kΩ. Higher concentration of nanotubes led to a slight increase in the strength of the material, which is due to the high strength of the nanotubes themselves and this allows using them as a reinforcing material.

Laser structuring of nanocomposite elements with MWCNT and silicone is one of the effective methods for modifying and improving the electrical characteristics of such nanocomposites. In our case, the electrical resistance decreases for all concentrations of MWCNT. At the same time, the samples were subjected to laser structuring of the same power and duration. The decrease in resistance is most likely due to the following factors. Laser structuring is caused by pyrolysis of the silicone matrix, which leads to the formation of gaseous particles which leave the material, thereby increasing the concentration of MWCNT and reducing the resistance of the material. Laser structuring leads to modification of nanotubes due to thermal effects, reducing the amount of impurities in MWCNT and the number of defects. Nanotubes can be sublimated and transformed to amorphous carbon, which will lead to a restructuring of MWCNT nets in a silicone matrix. Amorphous carbon can act as a solder and promote the formation of welded joints between individual nanotubes. All this may result in lower electrical resistance.

As a result of tensile tests, the strain sensitivity coefficient of the new nanocomposite MWCNT-based and silicone-based elements was found to have an average value of $S_l \sim 4.9$ (in the elongation range of 0–100,%) with a maximum value of 7 (at elongation of 100 %). These values significantly exceed the values of similar sensors published in the literature, where S_l, as a rule, does not exceed 2. At the same time, the designed elements demonstrate low hysteresis value < 3 %.

Figure 4, *a* shows a curve of the relative change in resistance versus relative elongation during stretching and relaxation of nanocomposite elements. The curve manifests a linear pattern of the system behavior. The curve (Fig. 4, *b*) shows the sample recovery rate when the active layer is stretched by 50,%. The curve shows that 4 s is required for the active layer to return to its initial resistance.

The ability of the prepared samples to withstand loads depends on their modulus of elasticity. When developing flexible wearable electronics designed for attachment to the human body, it is important to ensure comparability of the modulus of elasticity with the modulus of elasticity of the skin. For epidermis, this value was — (1.46 ± 0.26) MPa. The average modulus of elasticity of the manufactured nanocomposite tensoresistive elements was (1.1 ± 0.5) MPa. The experimental results also allowed to calculate the average tensile strength: (6.1 ± 0.5) MPa. Experimental data prove that when MWCNT is added to the Ecoflex silicone matrix it results in a 3 times higher strength.

2.3. Application of the designed nanocomposite tensoresistive elements for monitoring the motor activity

The designed nanocomposite tensoresistive elements in combination with a designed electronic unit can be used for monitoring of human motor function activity. Due to their flexibility, the samples make it possible to measure the deformation of body parts caused by anatomical movements (Fig. 5).

By attaching the element to the area under study, it is possible to determine the deformation directly in it. The resistance of the developed elements changes due to restructuring of the formed CNT net. By recording the changes in resistance of the elements, deformation is recorded. When deformation is removed, the resistance is restored, as the conductive net of nanotubes returns to its original morphology.

2.4. Gesture recognition

Based on the obtained nanocomposite tensoresistive elements, a smart sensor hand gesture recognition system was developed (Fig. 6). To do this, the electrically conductive sensors with electrodes connected to NI myRIO measuring

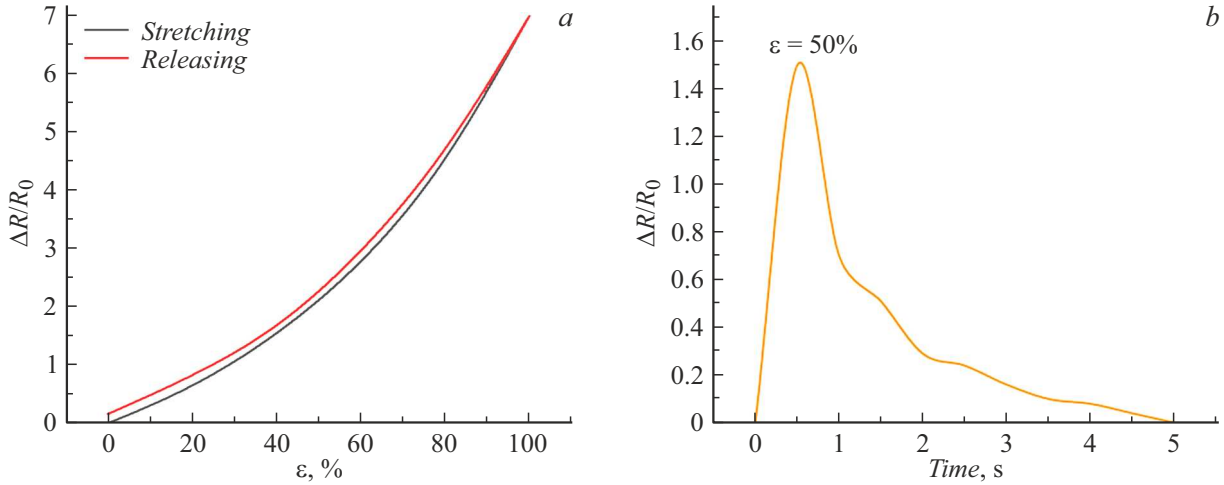

Figure 4. Dependence of the relative change in resistance at stretching and relaxation (*a*); recovery rate of the active layer at 50 % stretching (*b*).

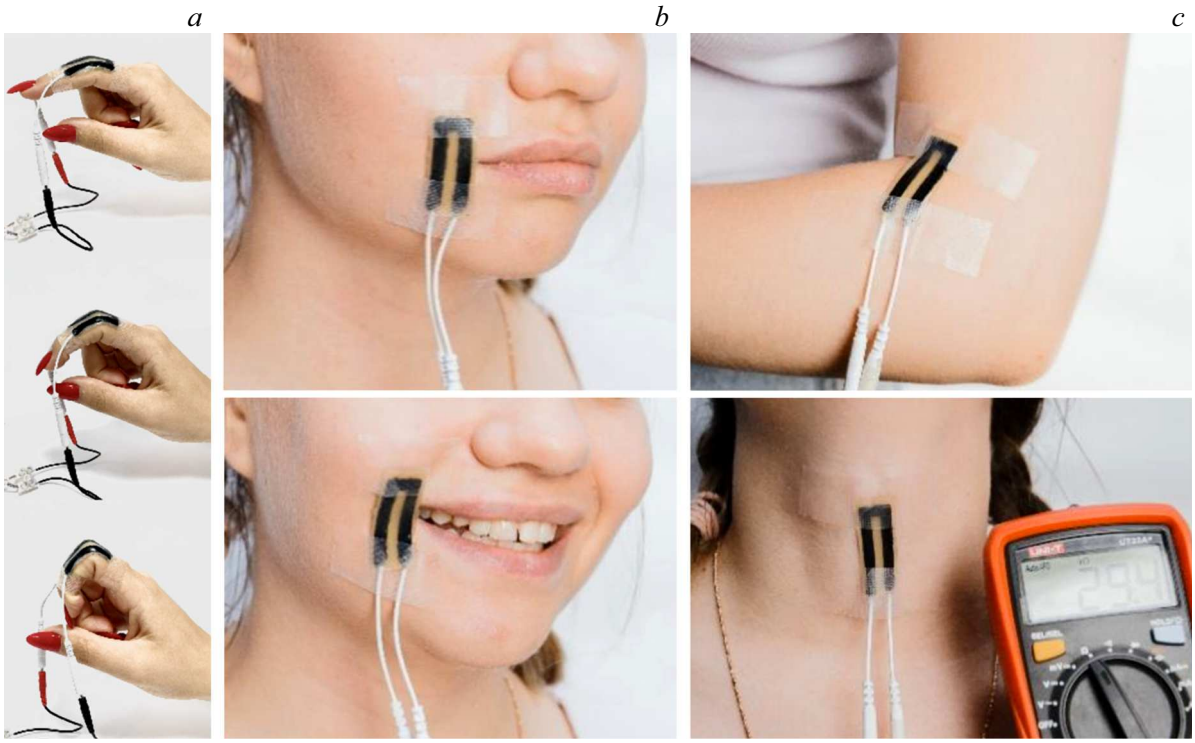

Figure 5. Measuring the deformation of body parts caused by anatomical movements: cyclic load on a composite tensoresistive element during bending (*a*) finger, (*b*) maxillofacial region, (*c*) elbow joint and larynx.

module were fixed to each finger in the movable joints using medical tapes. All five sensors reproducing the fingers conditions were arranged using gloves, as shown in Fig. 6, *a*. The feedback could be monitored on a PC connected to the measuring module (Fig. 6, *b*). The resulting smart gesture recognition system is shown in Fig. 6, *c*. The program for visualizing, reading and storing data, written in LabVIEW application framework, showed the graphs with real-time values of the sensors resistance amplitude, as well as „active/inactive“ status for all fingers of the hand. An example of a screenshot containing a program window on the computer is shown in Fig. 6, *d*.

For the experiment, data collected from nanocomposite tensoresistive elements were used, which measured the degree of resistance when the person made various gestures by hand. 11 different gestures were collected, including the basic gesture (fist) and 10 recognizable gestures. During the experiment, information about the gesture was displayed

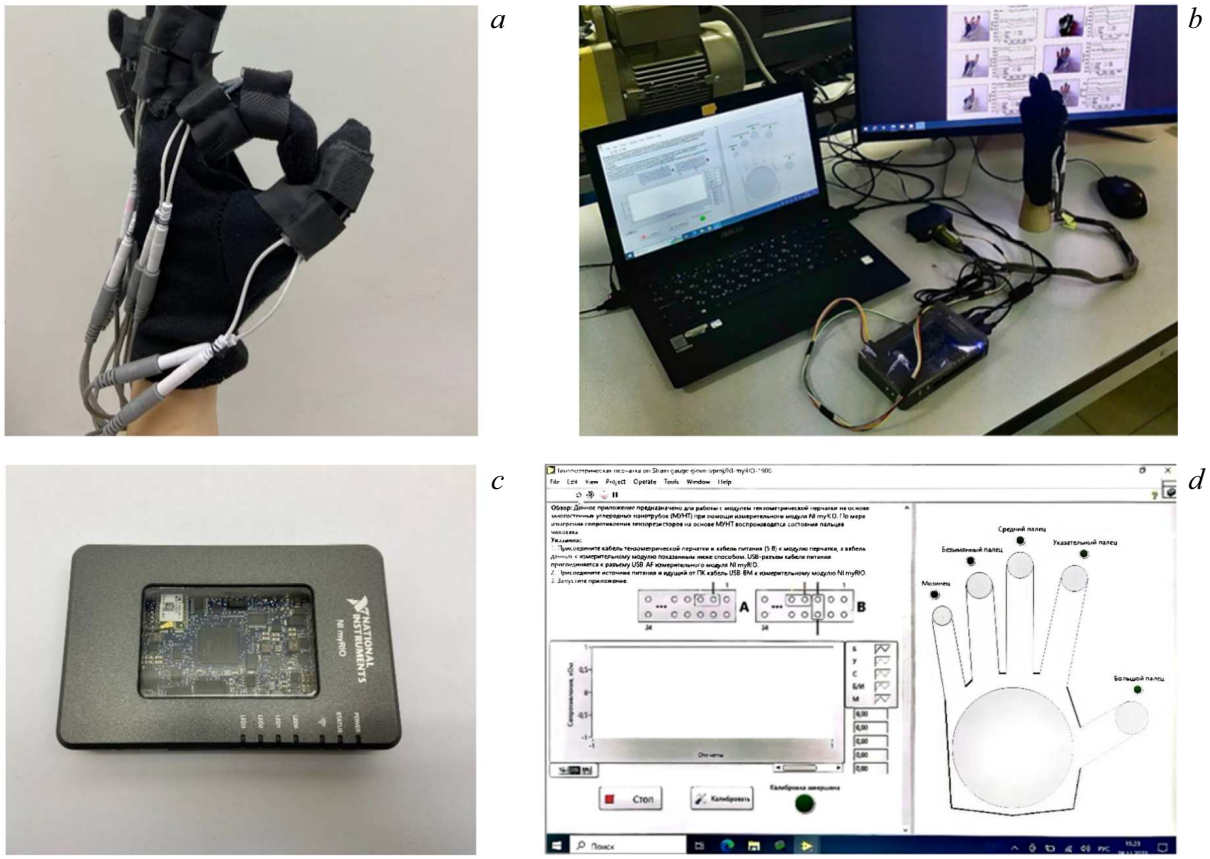

Figure 6. Smart sensor hand gesture recognition system: *a* — stationary nano-composite tensoresistive elements on the hand in the area of mobile knuckles in the form of a glove; *b* — smart hand gesture recognition system consisting of a glove with nano-composite tensoresistive elements and a measuring module; *c* — general view of the measuring module; *d* — application interface for reading and storing data from nanocomposite tensoresistive elements.

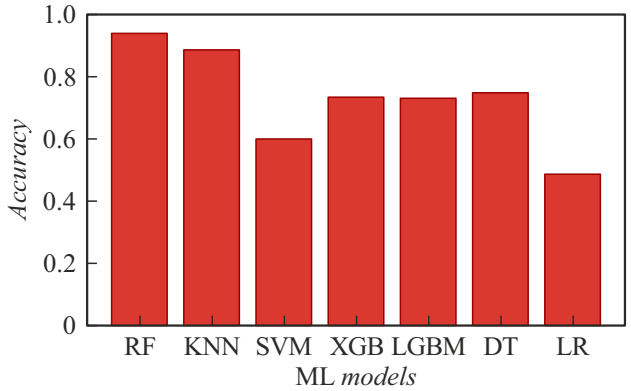

Figure 7. Accuracy for the next models of machine learning: classifier of k-nearest neighbors (KNN), support vector machine (SVM), classifier of random forest (RF), xgboost classifier (XGB), LightGBM classifier (LGBM), decision tree classifier (DT), logistic regression (LR) — when using a 105 string dataset for learning.

on the screen, while data from the sensors was recorded in a csv file with appropriate tag. Each gesture was measured for about 30 min, and the gesture that needed to be extended changed every 5 s. The data were recorded with the sampling frequency of 20 to 60 Hz. Seven different machine learning models were used in this work. Accuracy was used as a metric of the classification quality. Since learning of multiple models on the entire dataset is an extremely resource-intensive task, 105 strings from a dataset of 560,000 strings were used to compare the quality.y It was found that the use of a prepared smart system based on formed nanocomposite tensoresistive elements with conductive MWCNT nets made it possible to achieve high accuracy of gesture recognition $\sim 94\,\%$ (Fig. 7).

2.5. Detection of movements of the temporomandibular joint

The possibilities of using nanocomposite tensoresistive elements based on MWCNT nets for monitoring of temporomandibular joint (TMBJ) movements in orthopedic treatment in dentistry have been developed and investigated. For this purpose, models of jaws were made, plastered

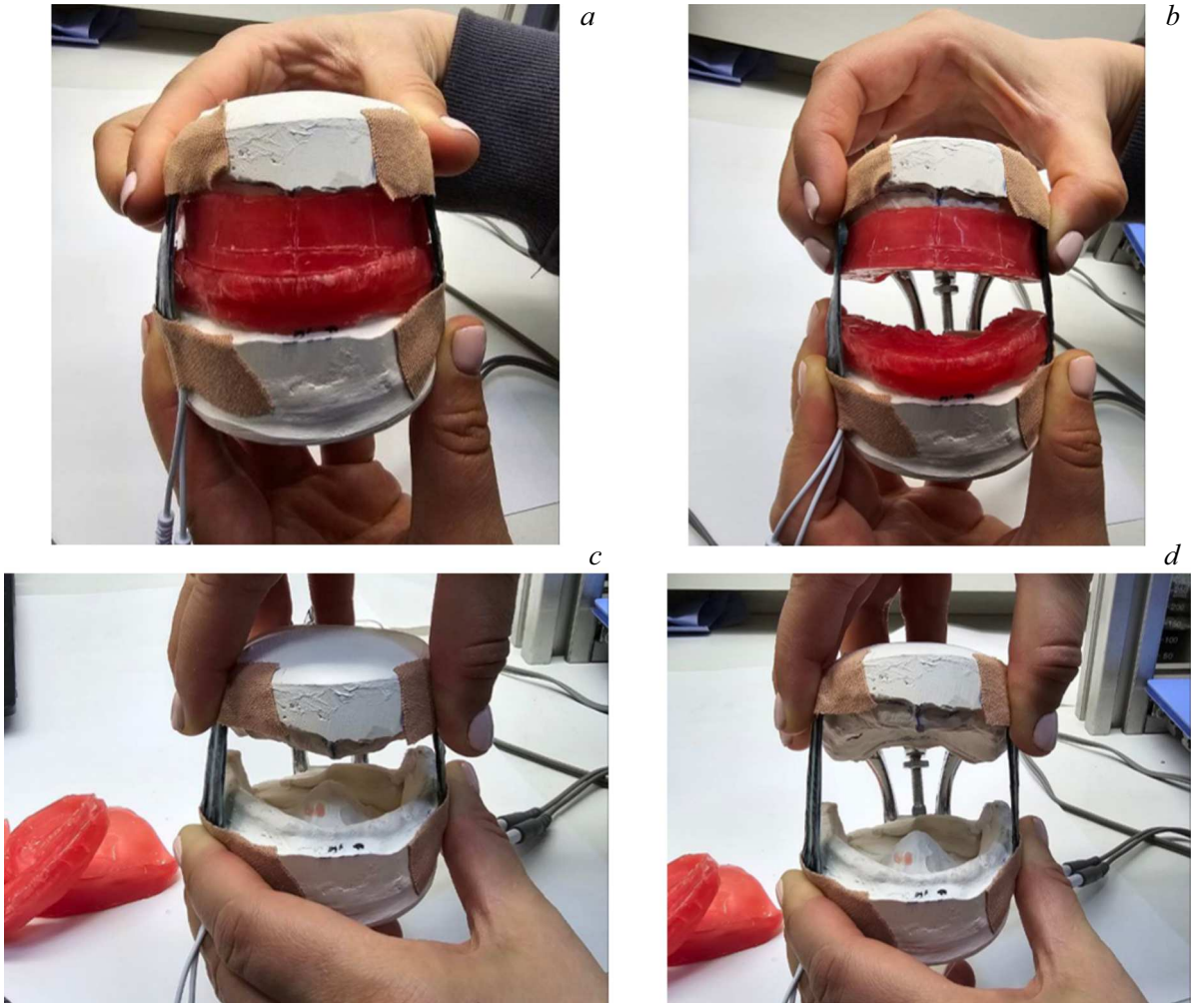

Figure 8. View of temporomandibular joint (TMBJ) with wax templates in closed (a) and opened (b) positions, view of TMBJ without wax templates in closed (c) and opened (d) positions.

into an bitelock with partial and complete adentia. The anatomical impressions from the upper and lower jaws with an alginate impression mass were made, the model was cast, wax bases were made, after which the central ratio of the jaws with occlusal rollers was determined and the jaws were centrally fixed with wax by conventional way.

The nanocomposite tensoresistive elements attached to the upper and lower jaw mockups made it possible to detect movements of the temporomandibular joint in the bitelock with full and partial adentia. View of temporomandibular joint (TMBJ) is provided with wax templates in closed and opened positions (Fig. 8, *a, b*), and view of TMBJ without wax templates in closed and opened positions (Fig. 8, *c, d*).

With TMBJ movement with wax templates (Fig. 9) and without them (Fig. 10), the change of relative resistance versus time for each of the nanocomposite tensoresistive elements (on the right and left parts of the TMBJ) are obtained. The movement of the TMBJ or the opening and closing of the biteblock was manifested by occurrence of a peak in the curves. A total of 9–10 peaks were obtained for each dependence, after which the average peak amplitude (β) was calculated, corresponding to the stretching of nanocomposite tensoresistive elements when finding the central ratio of the TMBJ.

The determined average values β, corresponding to the stretching of two nanocomposite samples on the right and left sides of the TMBJ during its opening/closing without wax templates, were $\beta 11 = (6.4 \pm 0.2)$ and $\beta 12 = (4.5 \pm 0.2)$. Average values β, corresponding to the stretching of two nanocomposite samples on the right and left sides of the TMBJ during its opening/closing with wax templates, were $\beta 21 = (4.4 \pm 0.2)$ and $\beta 22 = (3.6 \pm 0.2)$. Thus, the obtained values β correspond to the optimal value of TMBJ central ratio and should be observed by an orthopedic dentist and dental technician throughout the orthopedic treatment of partial or complete adentia. Since the implementation of such an orthopedic treatment process requires the use of expensive equipment and consumables to determine correct functioning of the TMBJ, and, consequently, the bite, the

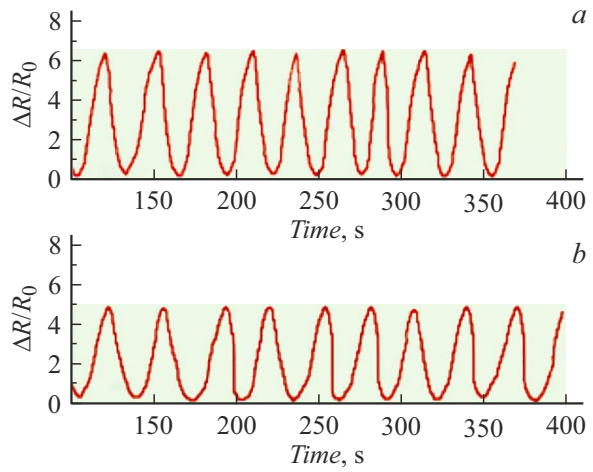

Figure 9. Time dependences of the relative resistance variation for each nano-composite element on the right (*a*) and left (*b*) parts of the TMBJ during its movement (opening/closing) without wax templates (full adentia).

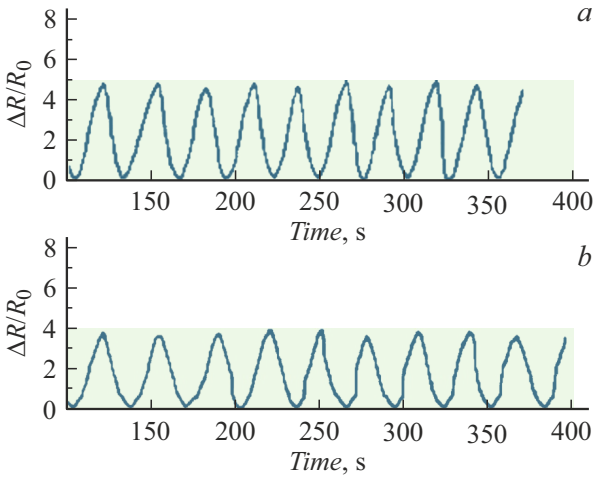

Figure 10. Time dependences of the relative resistance variation for each nano-composite element on the right (*a*) and left (*b*) parts of the TMBJ during its movement (opening/closing) with wax templates.

developed complex based on nanocomposite tensoresistive elements will save time and costs by removing the repeated treatment with wax templates, and will also reduce the likelihood of a medical error. Further improvement of the hardware and software of the complex will automate orthopedic treatment in dentistry and significantly save budget funds on materials and doctor's working hours.

Conclusion

The conducted studies prove the clearly observed strain-resistive properties of nanocomposites based on CNTs and biocompatible matrices. These materials exhibit the effect of electrical resistance variation during mechanical deformation, which makes them promising for creating the sensors for flexible electronics.

The nanocomposite tensoresistive elements based on MWCNT and Ecoflex silicone have been studied for use in the field of wearable electronics for motor activity monitoring. The presented samples are able to detect and respond to various forms of mechanical action, such as limb movements, gestures, and TMBJ movements.

As part of the study, the structural characteristics of nanocomposite tensoresistive elements were studied, their electrical conductivity and mechanical properties were evaluated, and their operability in various biomedical systems was tested. The results obtained allow to judge on the potential of using nanocomposite tensoresistive elements based on MWCNT and biocompatible matrices in medical applications.

Funding

The work was performed under the state assignment of the Ministry of Education and Science of Russia (Project FSMR-2024-0003).

Conflict of interest

The authors declare that they have no conflict of interest.

References

[1] Y. Jeong, J. Park, J. Lee, K. Kim, I. Park. ACS Sensors, **5** (2), 481 (2020). DOI: 10.1021/acssensors.9b02260
[2] Z. Zhang, X. Gui, Q. Hu, L. Yang, R. Yang, B. Huang, Z. Tang. Adv. Electron. Mater., **7** (7), 2100174 (2021). DOI: 10.1002/aelm.202100174
[3] M. Cianchetti, C. Laschi, A. Menciassi, P. Dario, Nat. Rev. Mater., **3** (6), 143 (2018). DOI: 10.1038/s41578-018-0022-y
[4] H.L. Park, Y. Lee, N. Kim, D.G. Seo, G.T. Go, T.W. Lee. Adv. Mater., **32** (15), 1903558 (2020). DOI: 10.1002/adma.201903558
[5] M.Z. Rahman, M. Rahman, T. Mahbub, M. Ashiquzzaman, S. Sagadevan, M.E. Hoque. J. Polym. Res., **30** (3), 106 (2023). DOI: 10.1007/s10965-023-03440-z
[6] J.J. Kim, Y. Wang, H. Wang, S. Lee, T. Yokota, T. Someya. Adv. Funct. Mater., **31** (39), 2009602 (2021). DOI: 10.1002/adfm.202009602
[7] A. Kumar. Sens. Actuators A: Phys., **344**, 113770 (2022). DOI: 10.1016/j.sna.2022.113770
[8] A. Kothuru, C.H. Rao, S.B. Puneeth, M. Salve, K. Amreen, S. Goel. IEEE Sens. J., **20** (13), 7392 (2020). DOI: 10.1109/JSEN.2020.2977694
[9] Y. Zhu, Y. Liu, Y. Sun, Y. Zhang, G. Ding. IEEE Sens. J., **22** (16), 15635 (2022).
[10] N.A. Demidenko, A.V. Kuksin, V.V. Molodykh, E.S. Pyankov, L.P. Ichkitidze, V.A. Zaborova, A.Y. Gerasimenko. Bioeng., **9** (1), 36 (2022) (in Russian). DOI: 10.3390/bioengineering9010036

[11] M. Kong, M. Yang, R. Li, Y.Z. Long, J. Zhang, X. Huang, C. Li, Int. J. Adv. Manuf. Technol., **131** (5), 3205 (2024). DOI: 10.1007/s00170-023-12007-7
[12] Y. Ren, X. Sun, J. Liu. Micromachines, **11** (2), 200 (2020). DOI: 10.3390/mi11020200
[13] Y. Wang, A. Liu, Y. Han, T. Li. Polym. Int., **69** (1), 7 (2020) (in Russian). DOI: 10.1002/pi.5907
[14] M. Lin, Z. Zheng, L. Yang, M. Luo, L. Fu, B. Lin, C. Xu. Adv. Mater., **34** (1), 2107309 (2022). DOI: 10.1002/adma.202107309
[15] H. Li, J. Zhang, J. Chen, Z. Luo, J. Zhang, Y. Alhandarish, L. Wang. Sci. Rep., **10** (1), 4639 (2020). DOI: 10.1038/s41598-020-61658-z
[16] H. Chi, L.J. Ze, X. Zhou, F. Wang. Dyes Pigm., **185**, 108916 (2021) (in Russian). DOI: 10.1016/j.dyepig.2020.108916
[17] A.Y. Gerasimenko, U.E. Kurilova, M.S. Savelyev, D.T. Murashko, O.E. Glukhova. Compos. Struct., **260**, 113517 (2021). DOI: 10.1016/j.compstruct.2020.113517
[18] A.V. Kuksin, O.E. Glukhova, A.Y. Gerasimenko. Semiconductors, **56** (13), 422 (2022). DOI: 10.1134/S106378262213005X
[19] A.Yu. Gerasimenko, O.E. Glukhova, G.V. Savostyanov, V.M. Podgaetsky. J. Biomed. Opt., **22** (6), 065003 (2017). DOI: 10.1117/1.JBO.22.6.065003
[20] A.Y. Gerasimenko, E. Kitsyuk, U.E. Kurilova, I.A. Suetina, L. Russu, M.V. Mezentseva, O.E. Glukhova. Polymers, **14** (9), 1866 (2022), DOI: 10.3390/polym14091866

Translated by T.Zorina